American Mineralogist, Volume 63, pages 1116–1136, 1978

Orthoferrosilite and other iron-rich pyroxenes in microperthite gneiss of the Mount Marcy area, Adirondack Mountains

HOWARD W. JAFFE, PETER ROBINSON AND ROBERT J. TRACY[1]

Department of Geology and Geography, University of Massachusetts Amherst, Massachusetts 01003

Abstract

Pyroxene–microperthite gneisses associated with anorthosite from the Mount Marcy area contain coexisting iron-rich orthopyroxene, augite, garnet, and hornblende, together with quartz, oligoclase, orthoclase, magnetite and ilmenite. Electron probe analyses of ferromagnesian silicates from the specimen with the most iron-rich coexisting pyroxenes gave the following compositions:

Orthopyroxene: $(Ca_{0.04}Mn_{0.04}Fe^{2+}_{0.92})(Fe^{2+}_{0.88}Zn_{0.01}Mg_{0.09}Fe^{3+}_{0.01})(Al_{0.02}Si_{1.98})O_6$

Augite: $(Na_{0.06}Ca_{0.83}Mn_{0.02}Fe^{2+}_{0.10})(Fe^{2+}_{0.85}Zn_{0.01}Mg_{0.07}Fe^{3+}_{0.04}Al_{0.03})(Al_{0.02}Si_{1.98})O_6$

Garnet: $(Ca_{0.66}Mn_{0.13}Fe^{2+}_{2.17}Mg_{0.01}Fe^{3+}_{0.04})(Fe^{3+}_{0.11}Al_{1.88})(Al_{0.03}Si_{2.98})O_{12}$

Hornblende: $(K_{0.38}Na_{0.48})(Na_{0.23}Ca_{1.77})(Mn_{0.05}Fe^{2+}_{3.82}Zn_{0.01}Mg_{0.23}Fe^{3+}_{0.43}Ti_{0.29}Al_{0.17})\cdot(Al_{1.81}Si_{6.19})O_{22}(OH)_2$

The orthopyroxene is the first documented natural occurrence of orthoferrosilite of space group *Pbca*. Lattice parameters (A) and optical properties of the orthoferrosilite as compared to synthetic $FeSiO_3$ are a = 18.42 (18.42), b = 9.050 (9.078), c = 5.241 (5.237), γ = 1.786 (1.789), β = 1.774 (1.780), α = 1.765 (1.772), $2V_{calc}$ = 79° + (86 °+). Analyses giving similar compositions have been recently reported from Norway and Canada.

Textural features of the rocks and exsolution lamellae in the pyroxenes and feldspars suggest the minerals equilibrated during the peak of Adirondack regional metamorphism and underwent exsolution and minor adjustment during subsequent cooling. Garnet in symplectic intergrowth with quartz and feldspar may have formed in part during cooling. The assemblages demonstrate great consistency in the distribution of elements between minerals, in particular, Fe/(Fe + Mg) of ilmenite = magnetite > garnet > orthopyroxene > hornblende > augite, and Mn/(Mn + Fe) of garnet > orthopyroxene > augite > hornblende ≅ ilmenite > magnetite.

The compositions of the pyroxenes in these rocks, together with analyses and optical data on fayalite-bearing assemblages from adjacent areas, permit estimates, based on experimental data, of temperature and pressure of metamorphism in the northeast Adirondacks. Absence of inverted pigeonite and compositions and distribution coefficients of coexisting augite and orthopyroxene suggest temperatures never exceeded 800°C. Exsolution features in pyroxenes and feldspars suggest the rocks cooled from above 600°C. Evaluation of the compositions of coexisting orthopyroxene–augite in terms of experimental work on the hedenbergite–ferrosilite join suggests a temperature of 760 to 790° for primary metamorphic crystallization and 600–660° for the temperature of fine exsolution. Depending on interpretation of the effects of minor constituents, the orthoferrosilite composition applied to various experimental data indicates that minimum pressures of metamorphism in the Mt. Marcy area were 7–9 kbar at 600°C or 9–11 kbar at 800°C. Fayalite-bearing assemblages from adjacent areas, evaluated using the same criteria, indicate maximum pressures of 7.5 to 9.5 kbar at 600° or 10–12 kbar at 800°C. These brackets and available experimental work on the Al_2SiO_5 polymorphs suggest metamorphism in the Mt. Marcy area took place near the high-pressure stability limit of sillimanite or in the kyanite zone.

[1] Present address: Department of Geology and Geophysics, Yale University, New Haven, Connecticut 06520.

0003–004X/78/1112–1116$02.00

Introduction

From their pioneering study of the system FeO–SiO_2, Bowen and Schairer (1932, p. 212, 230) concluded that "no crystalline compound of the composition, $FeSiO_3$, forms at any temperature where liquid occurs in the system, nor have we been able to find any evidence of its crystallization even at temperatures as low as 660° . . . All of the evidence thus points to the failure of formation of a compound of composition, $FeSiO_3$, in nature, just as it fails to form in synthetic mixtures." A few years later, Bowen (1935) identified and described a "ferrosilite" occurring as needles in the lithophysae of an obsidian from Kenya. From microscopic studies, he concluded that the mineral was clinoferrosilite. This was subsequently confirmed by Bown (1965), who measured lattice parameters for this mineral, established that its composition is close to Fs_{95}, and determined its space group to be $P2_1/c$. Experimental work by Lindsley (1965), Smith (1971a), and others indicated that orthopyroxenes richer in iron than Fs_{75}, in the so-called "forbidden zone" of the pyroxene quadrilateral, are stabilized relative to olivine plus quartz by high pressure. As a result, Smith (1971b) concluded that occurrences such as those described by Bowen must represent metastable crystallization, whereas many other occurrences of iron-rich orthopyroxenes are the result of magmatic and metamorphic processes at great depth. In this paper (see also Jaffe *et al.*, 1974, 1975) we present a complete documentation of a natural occurrence of orthoferrosilite ($Fs_{95.5}$, space group *Pbca*)[2] identified in pyroxene–microperthite gneiss[3] which is isoclinally folded with gabbroic anorthosite gneiss that forms the roof of the Marcy anorthosite massif in the Mount Marcy 15-minute quadrangle, eastern Adirondacks (Fig. 1). This and other reported natural occurrences of iron-rich pyroxenes are summarized in a histogram (revised from Smith, 1971a) in Figure 2.

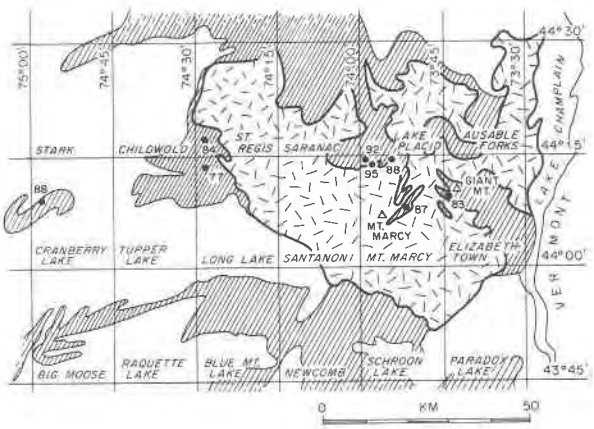

Fig. 1. Geologic index map of northeast Adirondack Mountains, New York showing Mt. Marcy anorthosite massif, and surrounding microperthite gneisses (ruled) and other rocks. Numbers at localities indicate the estimated Fs content [100 (Fe + Mn)/(Fe + Mn + Mg)] of iron-rich orthopyroxenes. The orthopyroxene rocks studied here are from the three localities near the north edge of the Mt. Marcy quadrangle. Olivine–augite gneiss FFG-6 is from close to the orthopyroxene locality "88" in the Cranberry Lake quadrangle.

The most iron-rich orthopyroxenes previously described from Adirondack gneisses (Fig. 1) include:

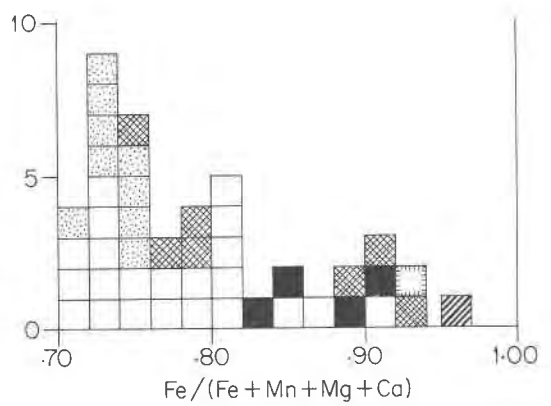

Fig. 2. Histogram of reported occurrences of iron-rich pyroxenes plotted according to the ratio Fe/(Fe + Mn + Mg + Ca) based on the data of Smith (1971a; also personal communication, 1975), Griffin and Heier (1969), this paper, Ormaasen (1977), and Klein (1978). Unmarked squares–orthopyroxenes reported previously; closed squares–analyses reported here; cross-hatched squares–orthopyroxenes reported by Ormaasen (1977); hachured square–orthopyroxene reported by Klein (1978); stippled squares–orthopyroxene coexisting with olivine; ruled square–clinoferrosilite in volcanic glass (Bowen, 1935; Bown, 1965) from Kenya.

[2] "Fs" expressed here as (100)(Fe + Mn)/(Fe + Mn + Mg). Griffin and Heier (1969) reported an electron probe analysis of an orthopyroxene with the composition SiO_2 45.6; Al_2O_3 0.2; MgO 2.6; FeO 50.8; CaO 0.7; Na_2O nil; MnO not determined, total 99.6, yielding $Fs_{91.6}$. While this paper was in revision following editorial review, complete electron probe analyses of orthopyroxenes from Lofoten, Norway were published by Ormaasen (1977). The most Fe-rich gave the composition SiO_2 45.93; TiO_2 0.05; Al_2O_3 0.14; FeO 50.16; MnO 2.39; MgO 0.43; CaO 0.62; Na_2O 0.14; yielding $Fs_{98.6}$. Comparably Fe-rich orthopyroxenes have been reported by Klein (1978) in metamorphosed iron formations from Canada.

[3] Rocks described herein as pyroxene–microperthite gneiss may be considered equivalent to those described from Adirondack terranes as charnockite or farsundite by de Waard (1970), as quartz syenite by Buddington (1969), or as quartz mangerite by Buddington (1972). Although some of these, such as the rock that forms the summit of Giant Mountain, are texturally granulites, by far the greater number are well foliated gneisses.

eulite (Fs_{77})[4] from pyroxene syenite gneiss of the Tupper-Saranac complex in the Long Lake quadrangle (Buddington and Leonard, 1962); eulite (Fs_{83}) in mafic pyroxene syenite gneiss and eulite (Fs_{84}) from syenite of the Tupper-Saranac complex (Davis, 1971), both in the St. Regis quadrangle; and eulite (Fs_{82} and $_{83}$) from charnockite in Roaring Brook valley on Giant Mountain (de Waard, 1970). Another occurrence outside the Mount Marcy quadrangle is of eulite (Fs_{88}, $\gamma = 1.776$) that we have found near Wanakena in the Cranberry Lake quadrangle. Indeed, iron-rich orthopyroxenes (Fs_{70-95}) are the rule, rather than the exception, in a large number of microperthite-rich gneiss samples collected from Pitchoff Mountain and Scott's Cobble, which make up the northern border of the Mount Marcy quadrangle and presumably extend into the Lake Placid quadrangle to the north. The experimental studies cited above show that the composition of orthopyroxene *in equilibrium with olivine plus quartz* at a given temperature is an indicator of pressure. In the absence of olivine in these rocks, the compositions of the orthopyroxenes indicate *minimum pressure* of metamorphism, which in the Mt. Marcy area appears to have been at least 7 kbar.

Buddington and Leonard (1962) reported the assemblage fayalite + quartz in fayalite–ferroaugite–microperthite "green granite" from near Wanakena, Cranberry Lake quadrangle in the west-central Adirondacks, about 80 km to the west of the Mount Marcy region. We report here a similar assemblage in sample FFG-6 collected from a new roadcut in this vicinity. The same assemblage was also reported by Kemp and Alling (1925) from quartz nordmarkite from the Ausable Forks quadrangle (Fig. 1), and this occurrence is further described by Buddington and Leonard (1962), who class the rock as "fayalite–ferrohedenbergite[5] granite." A specimen recently collected at this locality contains the same assemblage with an augite ($\gamma = 1.7645$) apparently identical to that in specimen FFG-6. Although these assemblages do not carry orthoferrosilite (or other orthopyroxene), their extremely high iron content suggests that they need not have formed at lower pressures of regional metamorphism.

The assemblage fayalite–ferroaugite–quartz is also well known from near-surface plutonic rocks. From the Nain, Labrador, intrusives emplaced deeper in the Earth's crust, perhaps at 10–20 km, Berg (1977) and earlier workers describe the assemblage eulite–fayalite–quartz–ferroaugite resulting from the breakdown of a single crystal of pigeonite. Similar assemblages have also been described by Bonnichsen (1969) in low-pressure, contact metamorphic rocks from the Dunka River area, Minnesota. Although inverted pigeonites have been recognized in anorthositic rocks by Davis (1971), and by Jaffe and Jaffe (unpublished) from rocks of the anorthositic series in the Mount Marcy quadrangle, there is no evidence of the crystallization of host grains of pigeonite in any of the pyroxene–microperthite gneisses described herein. Exsolution lamellae of pigeonite in host grains of ferroaugite that coexist with host grains of orthoferrosilite in these rocks represent relatively late, "low" temperature phenomena associated with waning phases of regional metamorphism (Jaffe *et al.*, 1975).

Tectonic setting

Buddington (1969) suggested that the Adirondack anorthosite series formed from a magma of gabbroic anorthosite liquid with a high percentage of suspended crystals of calcic andesine, and that flow differentiation accounted for the streaming and accumulation of plagioclase crystals resulting in a coarse megacrystic Marcy anorthosite core, bordered by an envelope or sheath of gabbroic anorthosite. He further noted that "screens" of metasedimentary gneisses commonly lie between the uppermost gabbroic anorthosite sequence and the pyroxene quartz syenite, and offered this as additional evidence for independent, subconformable, repetitive magma intrusion. De Waard (1970) believed that field and petrologic data favor the development of both the anorthositic and pyroxene–microperthite rocks from a single magma.

In the Mount Marcy quadrangle, detailed mapping by H. W. Jaffe, E. B. Jaffe and L. D. Ashwal shows a core of Marcy anorthosite overlain by gabbroic anorthosite, both showing textures believed to have originated from magmatic flow. Above these rocks discontinuous "screens" of calc-silicate marble, amphibolite, and other gneisses separate the anorthosite core from overlying rocks, which show a strongly developed gneissic fabric. The latter include (1) garnet–hornblende gabbroic anorthosite gneiss[6] with

[4] Buddington and Leonard (1962) report Fs_{82}; however, their γ index of 1.763 yields Fs_{77} according to the recent curve of Jaffe *et al.* (1975).

[5] For the purposes of this paper we use "ferroaugite" except where quoting directly from others.

[6] Analogous to the "transition rocks" of Buddington (1969) and the "Keene gneiss" of Kemp (1921) and Crosby (1966).

"xenocrysts" of plagioclase of varied An content, and (2) pyroxene–microperthite gneisses which carry iron-rich eulite and orthoferrosilite. These gneisses, along with intercalated calc-silicate marble and amphibolite, are interpreted to be involved in nappe structures developed during the diapiric rise of the anorthosite magma, as first suggested by Crosby (1966) in the adjacent Lake Placid and Ausable Forks quadrangles to the north. The high-pressure iron-rich orthopyroxenes may owe their origin to the development of the nappe structures associated with the regional metamorphism which affected all the Adirondack rocks and culminated at about 1150 m.y.

Petrography

In the field, the pyroxene–microperthite gneisses may be readily identified by their "maple-sugar brown" weathering surface (a function of the weathering of high-iron pyroxenes) and their strong gneissic foliation. Fresh surfaces, rarely seen in this area, are dark green. In other parts of the Adirondacks such rocks are classed as "green rocks," "green granites," and "green syenites." By contrast, the fayalite–ferrohedenbergite granite gneiss of the Wanakena area, Cranberry Lake quadrangle, weathers white rather than "maple-sugar brown." Evidently the well developed {100} partings and accompanying parallel (100) augite exsolution lamellae in host iron-rich orthopyroxenes provide channels for the pervasive entry of water during weathering, rendering eulite and orthoferrosilite more susceptible to weathering than fayalite.

Under the microscope the gneisses show elongate, discontinuous, mafic layers or lenses 1–5 mm wide, lying in a medium-coarse granoblastic felsic matrix consisting essentially of microperthite with minor hornblende, pyroxene, quartz, and plagioclase. The mafic lenses consist of weakly pleochroic eulite–orthoferrosilite and blue-green ferroan augite (0.3 × 1.0 mm), olive hornblende, magnetite, and ilmenite, along with relatively abundant, euhedral, colorless to pink, zoned to unzoned elongate zircon, and anhedral apatite. Intimate intergrowths of eulite–orthoferrosilite with ferroan augite on (100) simulate polysynthetic twinning under crossed nicols, and are a characteristic textural feature of these gneisses. We interpret the intergrowths in these rocks as the product of a thorough metamorphic recrystallization of an igneous precursor, and find no textural evidence to indicate that they resulted directly from exsolution from homogeneous augite or pigeonite at high temperature. Many of these mafic lenses are bordered by oligoclase-rich zones, and vermicular garnet–quartz rims occur abundantly along the contacts of plagioclase with pyroxenes or magnetite–ilmenite. Locally, euhedral garnet crystals nucleated in plagioclase very near the vermicular garnet. The felsic matrix is free of garnet and consists mainly of grains of untwinned or feebly twinned orthoclase microperthite to mesoperthite (1–5 mm). These show a microscopic braided texture with both coarse ribbons of uniformly oriented twinned sodic plagioclase and very fine strings or threads of sodic plagioclase. In some rocks, the orthoclase host has undergone ordering to produce microcline microperthite. Quartz (0.5–1 mm) is sporadic, as are grains of poorly twinned oligoclase.

Modes of the pyroxene–microperthite gneisses described here (Table 1) were determined by conventional point-counting (1000–1200 points) on standard thin sections. Quartz, microperthite, and ferrosilite content of orthopyroxene increase with decreasing color index and with generally decreasing anorthite content of plagioclase. This is a normal sequence of fractionation for rocks of igneous parentage. Buddington (1969, 1972) and Davis (1969, 1971) noted this trend and contrasted it with the trend of the anorthositic series, where the ferrosilite content of orthopyroxene increases *together with* the color index.

Electron probe analyses

Electron probe analyses of coexisting minerals were made on polished thin sections using the ETEC Automated Electron Probe at the University of Massachusetts, the MAC-400 Automated Electron Probe at Massachusetts Institute of Technology and, for a few earlier analyses, the MAC-400 at the Institute of Materials Science, University of Connecticut, Storrs. Corrections were done using the procedure of Bence and Albee (1968) and the data of Albee and Ray (1970). Eleven elements were routinely analyzed: Si, Ti, Al, Cr, Fe, Mn, Zn, Mg, Ca, Na, and K; Ba was analyzed only in a limited number of minerals.

The representative analyses in weight percent of oxides, given in Tables 4 through 8, were arrived at after thorough examination and computation of structural formulae for all analyses. In some cases an average of the best analyses from the entire group was used. This is noted at the bottom of each analytical column. For example, an average of the best three out of five analyses would be indicated "A3/5." In other cases we decided to select a single best analysis from the group. Thus the best of four would be indicated "1/4." Individual analyses of the coexisting

Table 1. Modes of pyroxene-microperthite gneiss

	Po-13	SC-6	Po-17	FFG-6
Quartz	4.1	9.1	13.8	18.4
Microperthite	37.2*	46.5*	52.6*	69.2**
Plagioclase***	32.7	25.1	18.2	3.5
Augite	6.2	8.7	6.6	3.7
Orthopyroxene	3.9	2.4	1.9	None
Olivine	None	None	None	0.6
Hornblende	3.8	2.1	4.1	3.9
Garnet	7.1	3.6	1.7	None
Magnetite + Ilmenite	3.0	1.9	0.8	0.5 Trace
Zircon	0.2	0.3	0.1	0.1
Apatite	1.8	0.3	0.1	0.1
	100.0	100.0	99.9	100.0
Color Index	26	19	15	9
Mole % An*** Plagioclase	23	16	18	11
Mole % Fs Orthopyroxene	85-88† 83-85††	92 89	95 91	
Mole % Fa† Olivine				99

Contains abundant exsolution lamellae of albite and is partially unmixed to microcline microperthite.

***A mesoperthite containing an oligoclase, An_{11} component.*

****An values for plagioclase host grains determined by measurement of the α index of refraction in oils. For probe analyses see Table 8.*

†100(Fe + Mn)/(Fe + Mn + Mg).

††100 Fe/(Ca + Fe + Mn + Mg) as used by Smith (1971a).

pyroxenes selected at an earlier time are published elsewhere (Jaffe *et al.*, 1975), and are not all identical with the analyses given here. Minerals are compositionally homogeneous, except for those discussed in detail below.

Mineralogy

Pyroxenes

The optical properties of eulite and orthoferrosilite are given in Table 2. The pleochroic scheme is the same for all three samples and the same as that of other members of the orthopyroxene series, but the intensity of pleochroism is weaker for these iron-rich members than for typical hypersthenes. The optic sign changes from negative to positive between ferrosilite contents of 88 and 92 percent, suggesting that a ratio of 100(Fe + Mn)/(Mg + Mn) = 90 may be a good division between eulite and orthoferrosilite on both optical and chemical grounds. All three iron-rich orthopyroxenes show strong dispersion accompanied by strongly anomalous birefringent colors in blues and browns, similar to those exhibited by iron-rich olivines.

The augites coexisting with these orthopyroxenes or with fayalite are also iron-rich, and all contain two or more sets of exsolution lamellae of pigeonite oriented on optimal phase boundaries that make irrational intercepts on the *a*− and *c*− crystallographic axes. The lamellae, except for those in the augite in specimen FFG-6, have been described in detail by Robinson *et al.* (1971a) and Jaffe *et al.* (1975). Augite in specimen FFG-6 has a pattern of pigeonite lamellae similar to that in augite Po-17, but no orthopyroxene lamellae were detected.

Lattice parameters derived from single-crystal X-ray photographs of orthoferrosilite from specimen

Table 2. Optical properties of iron-rich pyroxenes

	Po-13	SC-6	Po-17		$FeSiO_3$*
Orthopyroxenes					
γ	1.7763	1.785	1.786	Z=pale blue-green	1.789
β	1.7765	1.774	1.774	Y=pink-yellow	1.780
α	1.7560	1.764	1.765	X=pale pink	1.772
γ-α	0.0203	0.021	0.020		0.017
$2V_{calc.}$	88°,(-)	88°,(+)	79°,(+)		86°,(+)
Disp.	r<v,strong	r>v,strong	r>v,strong		
$\frac{Fe+Mn}{Fe+Mn+Mg}$	.88	.92	.95		1.00

	Po-13	SC-6	Po-17	FFG-6	Fe Augite**
Augites					
γ	1.7505	1.759	1.760	1.7645	(1.7646)
$\frac{Fe+Mn}{Fe+Mn+Mg}$	.83	.88	.93	.95	1.00

Indices as reported by Lindsley, Davis, and MacGregor, 1964. They report 2V = 58°(+) which is inconsistent with their indices.

***The value of γ for pure Fe augite is from the equation of Jaffe et al., 1975.*

Table 3. Lattice parameters of natural and synthetic orthoferrosilite

	Po-17	Synthetic $FeSiO_3$ Burnham (1965)	Sueno et al.(1973)
a (Å)	18.42	18.431	18.418
b (Å)	9.050	9.080	9.078
c (Å)	5.241	5.238	5.237
V (Å^3)	873.68	876.60	875.14

Po-17 are given in Table 3, together with two sets of lattice parameters for synthetic orthoferrosilite. The correspondence between the natural and synthetic material is close. X-ray single-crystal data on augites Po-13 and Po-17 and their exsolution lamellae are given by Jaffe *et al.* (1975).

For purposes of evaluation, the electron probe analyses of pyroxenes were recalculated on the basis of 4.000 cations, and an appropriate amount of Fe^{2+} was converted to Fe^{3+} to bring oxygen up to 6.000 (Table 4). The results of the Fe^{3+} calculations were irregular and unpredictable, commonly required assignment of Fe^{3+} to the tetrahedral positions, and were obviously dependent on minor variations in major oxide analyses, particularly SiO_2. Thus, calculated Fe^{3+} contents were ignored in all final graphical plots and all Fe was treated as Fe^{2+}. This approach seemed to give greater consistency in significant ionic ratios, suggesting that Fe^{3+} may be very minor.

One problem in interpreting the analyses is to see through the effects of fine exsolution lamellae that may have been analyzed inadvertently. Such effects are evident in the portion of the pyroxene quadrilateral shown in Figure 3, in which numerous analyses lie midway along tie lines between extreme compositions of orthopyroxene and augite. It seems evident that the extreme compositions are compositions of analysis locations where lamellae are scarce or absent, and represent compositions very close to those of host orthopyroxene and host augite. Use of a broad-beam analytical technique, such as has been used for some igneous pyroxenes to obtain bulk composition prior to exsolution, would produce inconsistent results because of the highly irregular distribution of lamellae as seen in thin section. As mentioned above, for the coarser (100) lamellae there is reason to believe that the intergrowths formed during metamorphic recrystallization rather than by precipitation from a homogeneous host.

A further problem exists in specimen Po-13, in which there are two distinct sets of homogeneous pyroxene analyses, Po-13A and Po-13B, that are lower and higher in Fe respectively. Petrographic examination shows that the low-Fe analyses are from layers or lenses in the specimen rich in garnet, whereas the high-Fe analyses are from layers or lenses about 1 cm away that lack garnet and are rich in hornblende. The possible significance of this and

Table 4a. Representative electron probe analyses of coexisting pyroxenes and olivine, and compositions of theoretical end members

	Po-13A	Po-13B	SC-6	Po-17	FFG-6	$CaFeSi_2O_6$
Augite						
SiO_2	47.81	47.84	48.51	48.69	47.66	48.44
Al_2O_3	1.31	1.17	1.00	1.00	.65	
TiO_2	.12	.10	.09	.14	.06	
Cr_2O_3	.05	.05	.00	.06	.03	
MgO	3.78	3.08	2.07	1.17	.91	
ZnO	.09	.07	.14	.19	.01	
FeO	25.73	26.75	27.68	29.18	29.14	28.96
MnO	.27	.38	.37	.43	.58	
CaO	19.54	19.92	19.43	19.07	20.32	22.60
BaO				.00		
Na_2O	.73	.72	.78	.72	.73	
K_2O	.00	.00	.00	.00		
Total	99.43	100.08	100.07	100.65	100.09	100.00
	1/3*	A5/10**	A4/10	A2/10	A5/16	
Orthopyroxene					Fayalite	$Fe_2Si_2O_6$
SiO_2	46.15	45.90	45.65	45.50	28.62	45.54
Al_2O_3	.30	.31	.27	.36	.08	
TiO_2	.06	.08	.13	.11	.00	
Cr_2O_3	.06	.02	.05	.06	.03	
MgO	4.62	3.52	2.48	1.36	.39	
ZnO	.28	.26	.38	.37	.31	
FeO	46.36	47.60	49.28	49.81	69.51	54.46
MnO	.51	.86	.72	1.10	1.57	
CaO	.80	.75	.79	.84	.05	
BaO				.06		
Na_2O	.00	.00	.00	.03		
K_2O	.00	.01	.00	.00		
Total	99.14	99.31	99.75	99.60	100.56	100.00
	A3/3	A3/8	A6/12	A11/26	A4/6	

**Selected best analysis out of 3.*

***Average of best 5 analyses out of 10.*

Table 4b. Structural formulae of coexisting pyroxenes and olivine and theoretical end members

	Po-13A	Po-13B	SC-6	Po-17	FFG-6	$CaFeSi_2O_6$
Augite						
Si	1.926	1.925	1.965	1.977	1.949	2.000
Al	.062	.056	.035	.023	.031	
Fe^{3+}	.012	.019			.020	
Total	2.000	2.000	2.000	2.000	2.000	2.000
Al			.013	.025		
Ti	.004	.003	.003	.004	.001	
Cr	.002	.002		.002	.000	
Fe^{3+}	.122	.124	.078	.044	.106	
Mg	.227	.185	.125	.071	.054	
Zn	.003	.002	.004	.006	.000	
Fe^{2+}	.733	.757	.860	.947	.871	1.000
Mn	.009	.013	.013	.015	.020	
Ca	.844	.859	.843	.830	.891	1.000
Na	.057	.056	.061	.057	.057	
Total	2.001	2.001	2.000	2.001	2.000	2.000
Orthopyroxene					Fayalite	$Fe_2Si_2O_6$
Si	1.969	1.971	1.969	1.980	.964	2.000
Al	.015	.016	.014	.019	.003	
Fe^{3+}	.016	.013	.017	.001	.033	
Total	2.000	2.000	2.000	2.000	1.000	2.000
Ti	.002	.003	.004	.004		
Cr	.002	.001	.002	.002	0	
Fe^{3+}	.025	.023	.022	.014	.036	
Mg	.294	.225	.159	.088	.019	
Zn	.009	.008	.012	.012	.007	
Fe^{2+}	1.613	1.674	1.739	1.798	1.892	2.000
Mn	.018	.031	.026	.041	.045	
Ca	.037	.035	.037	.039	.001	
Ba				.001		
Na				.003		
K		.001				
Total	2.000	2.001	2.001	2.000	2.000	2.000

Table 4c. Ionic ratios of coexisting pyroxenes and olivine and theoretical end members

	Po-13A	Po-13B	SC-6	Po-17	FFG-6	$CaFeSi_2O_6$
Augite						
$\frac{Fe}{Fe+Mg}$	.793	.829	.875	.933	.949	1.000
$Fe^{2+}/2.00$	.367	.379	.430	.474	.436	.500
$\frac{Fe+Mn}{Fe+Mn+Mg}$	.794	.832	.884	.934	.950	1.000
$\frac{Fe^{2+}+Mn}{Fe^{2+}+Mn+Mg}$	.766	.806	.875	.931	.943	1.000
$\frac{Fe}{Ca+Fe+Mn+Mg}$	.445	.460	.489	.520	.508	.500
$\frac{Ca}{Ca+Fe+Mn+Mg}$	.433	.439	.439	.435	.454	.500
$\frac{Ca+Mn+Na}{2}$	.455	.464	.459	.451	.484	.500
Orthopyroxene					Fayalite	$Fe_2Si_2O_6$
$\frac{Fe}{Fe+Mg}$	.849	.883	.918	.954	.990	1.000
$Fe^{2+}/2.00$	.807	.837	.870	.899	.946	1.000
$\frac{Fe+Mn}{Fe+Mn+Mg}$	.850	.885	.919	.955	.991	1.000
$\frac{Fe^{2+}+Mn}{Fe^{2+}+Mn+Mg}$	.847	.883	.915	.952	.990	1.000
$\frac{Fe}{Ca+Fe+Mn+Mg}$	.826	.855	.889	.915	.968	1.000
$\frac{Ca}{Ca+Fe+Mn+Mg}$	.018	.017	.019	.020	.000	0
$\frac{Ca+Mn+Na}{2}$	.028	.033	.032	.042		0
$K_D^{Opx-Aug}_{Mg-Fe}$	.681	.642	.668	.671	(.188)	

other inhomogeneities in the rocks is discussed later.

Detailed scrutiny of all 26 analyses of orthopyroxene from Po-17 demonstrates a slight bimodal and complementary distribution of MnO and MgO. One set has MnO from 1.19 to 1.48 weight percent (average 1.35) and MgO from 0.99 to 1.46 (average 1.25). The other set has MnO from 0.73 to 1.02 (average 0.88) and MgO from 1.26 to 1.82 (average 1.48). These minor fluctuations have virtually no effect on the ratio Fe/(Fe + Mg) and were ignored in obtaining the average analysis given in Table 4.

The chemistry of the pyroxene pairs is remarkably simple. If $MnSiO_3$ and $ZnSiO_3$ are added to the normal components of the pyroxene quadrilateral, $CaSiO_3$, $MgSiO_3$, and $FeSiO_3$, then 91 to 93 percent of the augites and 98.5 to 99 percent of the orthopyroxenes can be represented. In terms of the ratio Ca/(Ca + Fe + Mn + Mg) the "Wo" content of the augites coexisting with orthopyroxene (Table 4) ranges from 0.433 to 0.439 (average 0.437). For orthopyroxenes the same ratio ranges from 0.017 to 0.020 (average 0.019). Compared to more magnesian pyroxenes from the same area (Jaffe *et al.*, 1975), the Al contents are remarkably low, and little or no octahedral Al appears in the structural formulae. Al

is 3 to 4 times more abundant in augite than in orthopyroxene. The amounts of Ti and Cr are trivial in both pyroxenes. Calculated Fe^{3+}, though questionable, is almost twice as high in augite as in orthopyroxene, and augite has a consistently higher calculated Fe^{3+}/Fe ratio, in agreement with wet-chemical analyses of pyroxene pairs from elsewhere (Ashwal, 1974). The augite consistently shows about 0.06 Na atoms per formula unit. There is a fair correlation between Na and Al, but, because in the structural formulae all or most Al is assigned to tetrahedral sites, a jadeite substitution seems improbable. The calculated Fe^{3+} in octahedral sites is adequate to explain all Na in terms of an acmite component. The only other significant ions are Zn and Mn, both of which are approximately twice as abundant in orthopyroxene as in augite. Zn and Mn both tend to increase with increasing Fe/Mg ratio in the two pyroxene series, but the ratio Zn/(Zn + Mn) remains fairly constant between 0.13 and 0.33.

Fayalite

Olivine was analyzed in only one specimen, from the Cranberry Lake quadrangle, where it occurs in pale green, conchoidally-fractured crystals coexisting with augite but not with orthopyroxene. A representative analysis of this homogeneous mineral (Table 4) shows that it is about 97 percent Fe_2SiO_4, 2 percent Mn_2SiO_4, and 1 percent Mg_2SiO_4. Calculation based on stoichiometry, as in the case of the pyroxenes, suggests a modest amount of Fe^{3+}, but this may be entirely due to analytical error. Zn is roughly as abundant as in the orthopyroxenes, and is nearly half as abundant as Mg.

Garnet

Garnet tends to be concentrated in oligoclase-rich zones where it occurs in two habits, as vermicular intergrowths with quartz, and less commonly as small euhedral crystals in plagioclase. The vermicular intergrowths occur along contacts between plagioclase and pyroxenes, plagioclase and magnetite, and less commonly plagioclase and hornblende. Quartz occurs both within garnet and as thin rims around it. Small relics of plagioclase are commonly encased in the wormy quartz. In specimen Po-13 garnet and hornblende occur in different layers in the rock, but in the other specimens they are closely associated. Textural relations suggest garnet was the last mineral to form and is entirely of metamorphic origin.

The electron probe analyses of garnet (Table 5) were calculated to structural formulae based on 8.000

Table 5. Electron probe analyses and structural formulae of garnets

	Po-13		SC-6	Po-17	
	Euhedral	Symplectic		Euhedral	Symplectic
SiO_2	36.48	36.57	36.98	35,59	36.69
Al_2O_3	20.61	20.34	20.33	20.11	20.13
TiO_2	.05	.25	.05	.01	.05
Cr_2O_3	.01	-	.01	.00	.05
MgO	.66	.54	.40	.17	.08
ZnO	0	0	0	0	0
FeO	32.54	33.93	33.36	33.64	34.23
MnO	1.30	1.40	1.50	2.09	1.86
CaO	7.58	7.35	7.35	7.50	7.58
Na_2O	.00	-	.09	.09	.00
K_2O	.00	-	.00	.00	.00
Total	99.23	100.38	100.05	99.20	100.67
	A5/5	A3/5	A4/4	A3/3	A10/10
Si	2.970	2.955	2.993	2.915	2.967
Al	.030	.045	.007	.085	.033
Total	3.000	3.000	3.000	3.000	3.000
Al	1.949	1.893	1.934	1.857	1.883
Ti	.003	.015	.003	.001	.003
Cr	.001		.001		.003
Fe^{3+}	.047	.092	.062	.142	.111
Total	2.000	2.000	2.000	2.000	2.000
Fe^{3+}	.029	.020	.018	.100	.037
Mg	.080	.065	.048	.021	.009
Fe^{2+}	2.141	2.182	2.179	2.062	2.168
Mn	.089	.095	.104	.145	.128
Ca	.662	.636	.637	.658	.659
Na			.014	.014	
Total	3.001	2.998	3.000	3.000	3.000
Pyrope	2.7	2.2	1.6	.7	.3
Almandine	71.3	72.8	72.6	68.7	72.2
Spessartine	3.0	3.2	3.5	4.8	4.3
Grossular	20.5	16.6	19.0	18.6	17.4
Andradite	1.5	3.8	2.2	3.4	4.6
Other	1.0	1.4	1.1	3.8	1.2
$\frac{Fe^{2+}}{Fe^{2+}+Mg}$	.964	.971	.978	.990	.996
$\frac{Fe^{2+}+Mn}{Fe^{2+}+Mn+Mg}$	.965	.972	.979	.991	.996

Table 6. Representative electron probe analyses and structural formulae of hornblendes

	Po-13	SC-6	Po-17	FFG-6
SiO_2	38.68	38.38	37.96	38.32
Al_2O_3	10.26	10.08	10.27	9.01
TiO_2	2.11	2.43	2.37	1.90
Cr_2O_3	.02	0	.02	.05
MgO	2.64	1.51	.96	.71
ZnO	0	.12	.08	.10
FeO	28.62	30.13	31.15	32.62
MnO	.16	.21	.37	.36
CaO	10.40	10.13	10.11	10.36
Na_2O	2.23	2.22	2.26	1.86
K_2O	1.79	1.85	1.83	1.58
Total	96.91	97.06	97.38	96.87
	A9/14	A4/9	A8/11	A5/8
Si	6.255	6.252	6.191	6.295
Al	1.745	1.748	1.809	1.705
	8.000	8.000	8.000	8.000
Al	.211	.188	.165	.039
Ti	.257	.298	.290	.234
Cr	.003		.002	.007
Fe^{3+}	.345	.341	.431	.616
Mg	.636	.367	.233	.174
Zn	0	.014	.009	.012
Fe^{2+}	3.526	3.764	3.821	3.870
Mn	.022	.029	.049	.049
Total	5.000	5.001	5.000	5.001
Ca	1.802	1.768	1.767	1.825
Na	.198	.232	.233	.175
	2.000	2.000	2.000	
Na	.501	.469	.483	.416
K	.369	.384	.381	.332
	.870	.853	.864	.748
$\frac{Fe^{2+}}{Fe^{2+}+Mg}$	.847	.911	.943	.957
$\frac{Fe^{2+}+Mn}{Fe^{2+}+Mn+Mg}$	.848	.912	.943	.957
x*	.870	.853	.864	.748
y	1.073	1.125	1.178	1.130
w	.198	.232	.233	.175
z	1.745	1.748	1.809	1.705
x/x+y	.448	.431	.423	.398
w/x+y	.102	.117	.114	.093
x/z	.499	.488	.478	.439
$\frac{Fe^{3+}}{Fe\ Total}$	.089	.083	.101	.137

*Where $x = Na + K$ in $\underline{A}$ site, $y = R^{3+} + 2Ti^{4+}$ in (M1-2-3) sites, $w = Na$ in (M4), and $z = Al + Fe^{3+}$ in tetrahedral sites.

cations, in which Fe was assigned to Fe^{3+} to make a total of 24 positive charges. Resulting calculated Fe^{3+} and Fe^{2+} contents were used in all plots of garnet compositions. As expected, garnets have much higher ratios of $Fe^{2+}/(Fe^{2+} + Mg)$ than other coexisting ferromagnesian silicates, ranging from 0.964 to 0.996. In terms of end-member compositions, the garnets are dominated by almandine (71.3 to 72.8 percent) and grossular (16.6 to 20.5 percent). Andradite ranges from 1.5 to 4.6 percent. Pyrope content decreases systematically from Po-13 (2.7 percent) to Po-17 (0.3 percent), while spessartine increases in the same direction from 3.0 to 4.8 percent. Garnets of different habit in Po-17 have slightly different compositions. Euhedral garnets are richer in pyrope and poorer in almandine than the vermicular garnets of reaction rims. In the vermicular garnet of specimen Po-17 Mg is virtually a trace element, on a par with Ti, Cr, and Na.

Hornblende

Dark olive-brown hornblende occurs as distinct irregular grains, either isolated or associated with pyroxenes. The hornblende does not contain vermicular quartz or textural features commonly found in hornblende that has replaced pyroxene. Thus, on textural grounds, it is possible that the hornblende is a recrystallized igneous mineral.

Structural formulae calculated from electron probe analyses (Table 6) on the basis of 23 oxygens ("all ferrous") would show unreasonably large *A*-site occupancies and other improbable features. All formulae were recalculated and Fe^{3+} calculated on the basis of an ideal formula in which all Ca is assigned to the *M(4)* sites, and Mn and all smaller ions (Stout, 1971) are assigned to the *M(1-2-3)* sites (Robinson *et al.*, 1971b). Calculation of a greater amount of Fe^{3+} would force assignment of Ca to *M(1-2-3)* sites, which is structurally improbable. Alternatively Mn might have been assigned to *M(4)*, which would have resulted in a slightly higher *A* occupancy and lower Fe^{3+}.

On the basis of the calculated formulae, the hornblendes might be described as ferrohastingsites. Tetrahedral Al ranges from 1.705 to 1.809, and *A*-site occupancy from 0.748 to 0.870, of which 0.332 to 0.381 atoms per formula unit or 42 to 45 percent is K. From 0.175 to 0.233 Na atoms per formula unit substitute for Ca in the *(M4)* sites, as is common in most hornblendes. Substitutions of trivalent and quadrivalent ions for divalent ions in *M(1-2-3)* include 0.345 to 0.646 Fe^{3+}, 0.234 to 0.298 Ti^{4+}, 0.039

to 0.211 Al^{3+}, and up to 0.007 Cr^{3+}. There seem to be no systematic variations of these substitutions with Fe/Mg ratio, although hornblende FFG-6 has lower tetrahedral Al, *A*-site occupancy, and Ti, and higher Fe^{3+} than the other three. In terms of tetrahedral Al and *A* occupancy, these hornblendes have much higher calculated *A*-site occupancy than the "ideal hornblende" trend described by Robinson *et al.* (1971b). They are like many other reported high *A*-site hornblendes from igneous and granulite facies environments in being rich in Fe^{2+}, in Fe^{3+} and in K (Buddington and Leonard, 1953; Henderson, 1968; Leelanandam, 1970). Although we did not analyze for F and Cl, petrologic arguments, as well as published analyses of hornblendes from similar Adirondack rocks (Buddington and Leonard, 1953), suggest that these elements may be present in significant amounts.

Ilmenite and magnetite

Ilmenite and magnetite in the Mt. Marcy specimens occur as relatively coarse discrete irregular grains, commonly in close association with each other and with ferromagnesian silicates. Both minerals are remarkably free of exsolution lamellae. Analyses of ilmenites from all three orthopyroxene-bearing rocks (Table 7) are essentially the same and consist in mole percent of 90.2 to 92.6 percent $FeTiO_3$, 6.5 to 8.8 percent Fe_2O_3, and 0.8 to 0.9 percent $MnTiO_3$. Analyses of magnetites from Po-13 and Po-17 are also extremely similar and consist, in mole percent, of 96.9 to 98.3 percent $Fe^{2+}Fe^{3+}_2O_4$, 2.2 to 0.7 percent $Fe^{2+}_2Ti^{4+}O_4$, and 0.9 percent $FeAl_2O_4$. Mn is present in very minor amount in both and is slightly enriched in magnetite from Po-17. When magnetite and ilmenite compositions are applied to the data of Buddington and Lindsley (1964) and Lindsley and Rumble (1977), they suggest equilibration at 520–600°C and at f_{O_2} of 10^{-17} to 10^{-20}. This temperature estimate suggests that the oxides re-equilibrated at a temperature below the maximum thermal peak of metamorphism as estimated from silicate assemblages.

Preliminary observations and probe analyses (not given here) of the oxides in specimen FFG-6 indicate preservation of fine exsolution lamellae of ilmenite in magnetite, and hence far less metamorphic re-equilibration than in the case of the Mt. Marcy specimens. Preliminary composition estimates of $Mag_{70}Usp_{30}$ and $Ilm_{95}Hem_5$ suggest equilibration at 670°C and $f_{O_2} = 10^{-18}$ near the QFM buffer. Analyses of bulk oxide separates from the same rock type and locality by Buddington and Lindsley (1964) suggested 765°C and $f_{O_2} = 10^{-13.8}$ as the conditions of primary crystallization [or 820°C and $f_{O_2} = 10^{-12.4}$ when replotted on the new graph of Lindsley and Rumble (1977)].

Table 7. Representative electron probe analyses and structural formulae of ilmenites and magnetites

	Po-13	SC-6	Po-17		Po-13	SC-6	Po-17
Ilmenites							
SiO_2	0	0	0	Al	.002	.003	.000
Al_2O_3	.08	.11	.01	Ti	.923	.935	.912
TiO_2	48.22	48.02	47.78	Cr	-	.000	-
Cr_2O_3	-	.01	-	Fe^{3+}	.075	.062	.088
MgO	0	0	0	Total	1.000	1.000	1.000
ZnO	0	0	0	Fe^{3+}	.077	.065	.088
FeO	50.08	48.60	50.79	Fe^{2+}	.915	.926	.902
MnO	.35	.39	.40	Mn	.008	.009	.009
CaO	.01	0	.03	Ca	.000	0	.001
Total	98.74	97.13	99.01	Total	1.000	1.000	1.000
	A3/12	A3/8	1/7				

	Po-13	Po-17		Po-13	Po-17
Magnetites					
SiO_2	0	0	Al	.017	.018
Al_2O_3	.38	.40	Ti	.022	.007
TiO_2	.76	.25	Fe^{3+}	1.937	1.965
MgO	0	0	Fe^{2+}	.024	.010
ZnO	0	0	Total	2.000	2.000
FeO	92.88	92.59	Fe^{2+}	.998	.994
MnO	.05	.11	Mn	.002	.004
CaO	.01	.06	Ca	.001	.003
Total	94.09	93.41	Total	1.001	1.001
	1/3	A3/6			

Feldspars

Textural relations and probe analyses of feldspars (Table 8) from all three orthopyroxene-bearing specimens suggest the same complex history. Cores of discrete plagioclase grains, presumed to represent original maximum temperature plagioclase, are An_{18} to An_{20}. Original orthoclase is now represented by a complex microperthite, the original bulk composition of which would have to be determined by detailed modal analyses. At least two stages of exsolution are recognized. The first stage is represented by discrete blebby lamellae of plagioclase An_{13} to An_{15}. This exsolution effectively depleted the host of nearly all the anorthite component. The remaining host consists of

Table 8. Representative compositions of feldspars determined by electron probe analyses

		Po-13	SC-6	Po-17
Plagioclase	An	.193	.201	.182
Core	Ab	.798	.785	.802
	Or	.009	.014	.016
		A3/5	1/3	1/9
Coarse	An	.138	.153	.144
Plagioclase	Ab	.856	.842	.851
Lamellae in	Or	.006	.005	.005
K-feldspar		A2/2	1/1	1/1
Plag. Lam.	An		.144	
in Ksp. near	Ab		.841	
Garnet	Or		.014	
Symplectite			1/2	
Plagioclase	An	.010	.082	
Rims	Ab	.986	.911	
	Or	.004	.007	
		1/11	1/3	
K-feldspar	An			.007
Rich in	Ab	.334		.296
Albite	An	.666		.698
Lamellae		1/5		1/1
Clean	An		.004	.003
K-feldspar	Ab	.103	.100	.125
	Or	.897	.896	.872
		1/5	A3/5	1/2
Clean	An		.003	
K-feldspar	Ab	.067	.093	
near Garnet	Or	.933	.908	
Symplectite		1/2	1/1	

orthoclase with variable amounts of very fine lamellae. Where lamellae are abundant the host composition ranges from $Or_{84}Ab_{16}An_0$ to $Or_{66}Ab_{34}An_0$. Areas free of lamellae have a composition of Or_{88-90}. These data indicate that the last phase of exsolution involved separation of pure or nearly pure albite which moved the remaining host composition from a somewhat more sodic composition to about Or_{90}. Analyses of discrete plagioclase grains suggest they were overgrown by more sodic material derived during both stages of exsolution of plagioclase from orthoclase, most abundantly by An_{13-15} provided during the first coarse exsolution, but in some cases by extremely thin edges that are pure albite.

Analyses of feldspars enclosed by quartz in or adjacent to vermicular garnet give some insight into the timing of garnet growth. Plagioclase is An_{14-15}, coincident in composition with blebby lamellae in orthoclase, and orthoclase is Or_{90-93}, similar to the cleanest host orthoclase. Although the exact interpretation of the feldspar compositions is not clear, these data support textural evidence that garnet growth was late and may have taken place as the rocks cooled below the metamorphic maximum.

Mineral assemblages

As far as can be determined in thin section, all the minerals listed in the modes of these rocks (Table 1) are in mutual contact at one place or another and appear to constitute an approach to an equilibrium metamorphic assemblage. Possible exceptions to this are the symplectic garnet intergrowths that in places form vague coronas, suggesting garnet-forming reactions that have not attained equilibrium. Another exception is the obvious evidence of intracrystalline re-equilibration in pyroxenes and alkali feldspars since the metamorphic peak, which has locally caused composition changes in adjacent minerals, such as the late albitic rims on some plagioclases. When differences in mineral compositions from single thin sections, particularly pyroxenes in Po-13, are compared with textural evidence for vague compositional layers and lenses (see above), it becomes evident that true equilibration took place on a scale considerably smaller than that of a single thin section. In spite of this, it seemed worthwhile to treat the rocks as if they do represent equilibrium mineral assemblages, and to see what regularities and irregularities this approach would bring out.

All the orthopyroxene-bearing specimens, Po-13, SC-6, and Po-17, were collected within 5 km of each other in the northern part of the Mt. Marcy quadrangle and hence can be considered to have attained essentially the same P–T conditions during regional metamorphism. Specimen FFG-6, collected for comparative purposes from the Cranberry Lake quadrangle about 100 km away, may or may not have been metamorphosed under the same conditions.

Chemographic relations

Pyroxene quadrilateral

The compositions of the coexisting pyroxenes and olivine are shown in terms of the pyroxene quadrilateral in Figure 3. The extreme compositions of pyroxenes on the tie lines, as well as the analyses in Table 4, probably represent the compositions of host augite and host orthopyroxene after the exsolution had taken place subsequent to the peak of metamorphism. In these particular rocks we find it difficult to make estimates of the compositions of coexisting py-

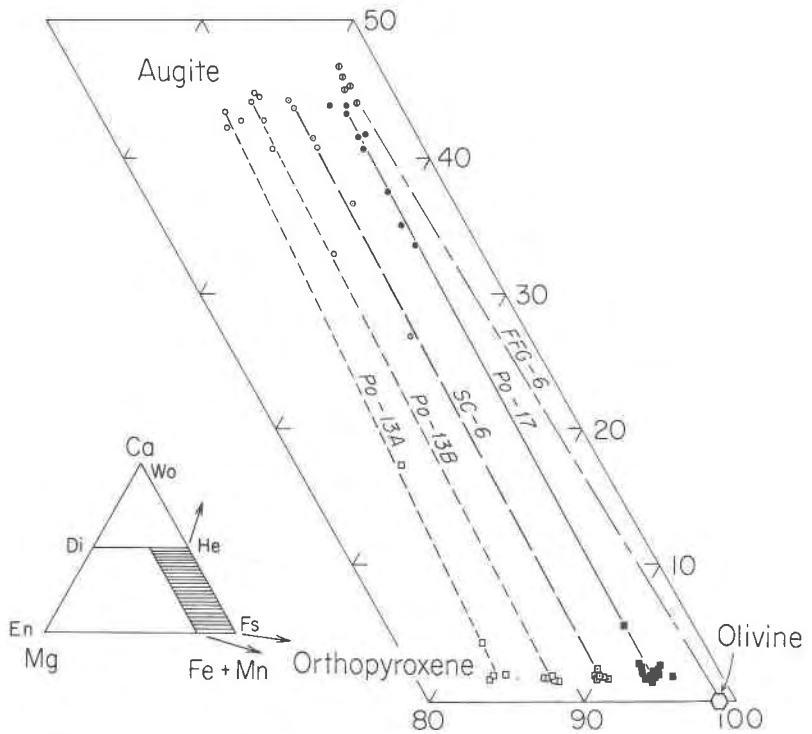

Fig. 3. Iron-rich portion of the pyroxene quadrilateral showing representative analyses of coexisting augite and orthopyroxene, and augite and olivine. Analyses that lie midway along tie lines are where various proportions of fine exsolution lamellae were analyzed inadvertently. Extreme compositions are of analysis locations where lamellae are scarce or absent, and represent compositions very close to those of host orthopyroxene and host augite.

roxenes at the peak of metamorphism. We believe these gneissic rocks have been thoroughly reconstituted from their igneous precursors, but that the metamorphic pyroxenes, even at the peak of metamorphism, may have been rather complex and irregular intergrowths. Although crude, the best estimates of primary metamorphic augite compositions that we have are based on X-ray single-crystal photographs of augites Po-13 and Po-17 (Jaffe *et al.*, 1975, Table 4) that suggest they contain approximately 15 percent of pigeonite and orthopyroxene lamellae.

The Wo content of augites is most commonly expressed, as it is in Figure 3, by the ratio Ca/(Ca + Mn + Fe + Mg). However, we feel it is misleading to compare Wo contents of natural pyroxenes expressed in this way with Wo contents of experimentally-produced augites in the pure system $CaSiO_3$–$MgSiO_3$–$FeSiO_3$. In the pure system the temperature-sensitive ratio Ca/(Ca + Fe + Mg) of augite is in inverse relation to the amount of small cations Mg and Fe substituted into the *M(2)* site, normally dominated by the large cation Ca. To express the Wo compositions of natural pyroxenes in a way which will take into account all large cations, will indicate correctly the amount of small cations substituted in *M(2)*, and will provide better direct comparison with experimental work in the pure system, we suggest the sum of Ca + Na + Mn in the structural formula divided by two [(Ca + Na + Mn)/2]. On the basis of Ca/(Ca + Mn + Fe + Mg), the Wo contents of host augites and host orthopyroxenes range from 0.433 to 0.439 (average 0.437) and 0.017 to 0.018 (average 0.019) respectively. On the basis of (Ca + Na + Mn)/2 the same analyses yield Wo contents from 0.451 to 0.464 (average 0.457) and 0.028 to 0.042 (average 0.034). These are the values that should be compared with experimental work to estimate the temperature at the end of the episode of fine exsolution. From these average values and the estimate of 15 percent pigeonite and orthopyroxene lamellae in augite, the original "homogeneous" Wo composition of metamorphic augite is estimated as Ca/(Ca + Mn + Fe + Mg) = 0.374 or (Ca + Na + Mn)/2 = 0.393, reasonable values in light of experimental data for high-*T* granulite-facies conditions (Lindsley *et al.*, 1974).

In our analyses there appears to be no systematic relation between Wo content of coexisting pyroxenes and Fe/Mg ratio, but this is not surprising in view of

the narrow range of Fe/Mg ratios considered. However, a much wider range of pyroxene pairs from the Mt. Marcy area, reported elsewhere (Jaffe *et al.*, 1975) also shows very little variation in Wo content with Fe/Mg ratio, in spite of the fact that the more magnesian augites have roughly twice the Al_2O_3 content and the orthopyroxenes 2 to 5 times the Al_2O_3 contents of the iron-rich pyroxene pairs reported here. Because the Wo contents reported here are not a function of Fe/Mg ratio, the average values can be projected to the hedenbergite–ferrosilite join of Lindsley and Munoz (1969), and compared with their experimental data (see below).

The augite coexisting with olivine has a Wo content about 2 percent higher (0.454 or 0.484) than the augites in orthopyroxene assemblages (0.437 or 0.457), consistent with the metastability of orthopyroxene with respect to fayalite–quartz. Further, the augite–olivine tie line lies at a more iron-rich composition than any of the pyroxene pairs, and is not in conflict with the possibility that specimen FFG-6 equilibrated under identical conditions. Although no quartz–olivine–orthopyroxene–augite assemblage has yet been located, the data in Figure 3 permit one to visualize what the equilibrium three phase field *might* look like, with a width less than Fe/(Fe + Mg) = 0.045. Although the exact position of the equilibrium three-phase field is not known, the composition of the orthopyroxene in Po-17 can be used to estimate *minimum* pressure, and the composition of olivine in specimen FFG-6 can be used to estimate *maximum* pressure, on the basis of available experimental data.

ACF projection

In Figure 4 the average compositions of ferromagnesian silicates from Tables 4, 5, 6, and 7 are plotted in a modified ACF diagram using cation rather than oxide ratios. The A apex includes not only Al^{3+} but any other substituting trivalent ion such as Fe^{3+}[7] and Cr^{3+}. Each Ti^{4+} ion is combined with an Fe^{2+} to create *two* "mean" trivalent ions (*i.e.* "2 Ti"), and thus an amount of Fe^{2+} equivalent to 1 Ti is subtracted from the F total. The A total is also reduced to the extent that trivalent ions are compensated for by the mono-

[7] As stated elsewhere calculated Fe^{3+} values were accepted for garnet and hornblende, but rejected for pyroxenes.

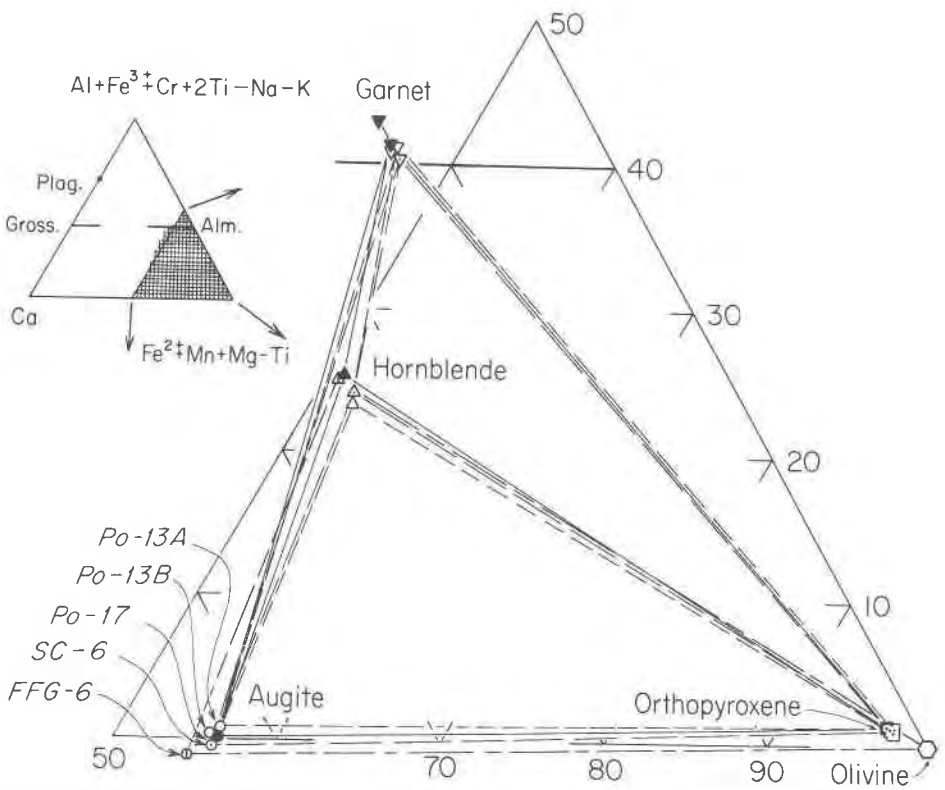

Fig. 4. Modified ACF plot of ferromagnesian assemblages. Compositions of minerals in four different rocks, including FFG-6 with olivine and without garnet, show great regularity.

valent ions Na and K. In effect this removes from portrayal jadeite and acmite in pyroxenes, and various Na,K substitutions in amphiboles, leaving only the pure Tschermak's-type substitutions (*i.e.* $[Al, Fe^{3+},Cr,Ti]^{VI} + Al^{IV} \rightarrow [Mg,Fe^{2+}]^{VI} + Si^{IV}$). Since quartz is present in all assemblages, Figure 4 is considered a silica-saturated phase diagram.

In plotting pyroxene compositions, the calculated Fe^{3+} contents were ignored, which leads to slightly lower but less erratic A than would otherwise be the case. Both augite and orthopyroxene analyses plot near or below the 0 percent A line, showing how trivial Tschermak's-type substitutions are, although these pyroxenes are all Al-saturated in the presence of garnet. In the garnets, where calculated Fe^{3+} values were used in plotting, there is amazing consistency between the three rocks, and all analyses fall close to a point representing 21.5 percent grossular + andradite and 78.5 percent of combined almandine, spessartine, and pyrope. These values compare with the values of about 15 percent and 85 percent determined in garnets synthesized in coexistence with aluminous augite and aluminous orthopyroxene at 1200°C and 30 kbar in the system $CaSiO_3$–$MgSiO_3$–Al_2O_3 (Boyd, 1970, Fig. 14). Hornblendes, in which calculated Fe^{3+} was used in plotting, do show consistent grouping, very close to the augite–garnet tie line. When examined as a whole, no significant differences between the three orthopyroxene assemblages show up on the modified ACF diagram.

Behavior of Mn

One problem related to comparisons of natural and experimentally produced pyroxenes in the quadrilateral is the behavior of Mn, particularly for iron-rich compositions (Lindsley *et al.*, 1974). Mn was added to Fe in plotting analyses in Figure 3. In Figure 5a all other ions were ignored and pyroxenes and olivines as well as garnets and hornblendes were plotted on the basis of Mn, Mg, and Fe^{2+}. Among the pyroxenes, the orthopyroxenes consistently show a higher Mn/Fe ratio than augites, and both sets of pyroxenes show a consistent trend of increasing Mn with increasing Fe/Mg ratio. The most Mn-rich orthopyroxene plotted shows nearly 3 percent of the Mn end member. The average orthopyroxene in Po-17 (Table 4), taking into full account all substitutions, has about 2 percent $MnSiO_3$. The olivine shows lower Mn than an extension of the pyroxene trend, consistent with the data of Lindsley *et al.* (1974), Huntington (1975), and Berg (1977). The actual amount of Mn_2SiO_4 is about 2 percent. The hornblendes show a lower Mn/Fe ratio than the other coexisting silicates. As expected, the garnets have a higher Mn/Fe ratio than all other minerals, and in addition are all very low in Mg. The oxides come very close to being Fe^{2+} end members, with minor Mn and no Mg.

Note in Figure 5a that in specimen Po-17 *all* of the silicates still lie between 91 and 95 percent of the Fe apex, and in all of the minerals except garnet, Mg is more important than Mn. Thus, although Mn clearly does have some effect on the stability relations of Fe-rich orthopyroxenes and olivines, the amounts of Mn involved are relatively slight, and the differences between orthopyroxenes and olivine are even more slight.

Plagioclase projection

The ACF diagram of Figure 4 does not portray the different Mg and Fe + Mn contents of the ferromagnesian minerals, but it may be expanded by splitting the F apex into Mg and Fe + Mn apices, permitting treatment in three dimensions in an ACFM tetrahedron. Phase relations in such a tetrahedron may be viewed in two dimensions by means of a plagioclase projection, as was done by Robinson and Jaffe (1969). They showed that the projection is a valid phase diagram so long as plagioclase is present and changes in plagioclase composition have no effect on the relations of the other phases. Figure 5b is such a plagioclase projection, onto the CFM plane, of the ferromagnesian silicate assemblages considered here, modified into a more convenient rectangular form. Figure 5c is a similar projection, but in which the original F apex has been split differently into Fe + Mg and Mn components. The similar or overlapping three-phase triangles for orthopyroxene–augite–garnet in both Figure 5b and Figure 5c are a sure indication that the original F apex cannot be successfully split into just two determining inert components, but that Fe, Mg, and Mn must all be treated separately. This can be done in a three-dimensional representation that is a combination of all three parts of Figure 5, as shown in Figure 6. In Figure 6 we see that there is no crossing or overlap of orthopyroxene–augite–garnet tie planes, that MnO is an essential component (see also Fig. 5c) and appears to explain the presence of garnet in these rock compositions, and that the Fe/Mg ratio has no influence on the mineral assemblage provided the bulk composition (as projected) lies within the triangular prismatic volume defined by the three-phase tie planes. Figure 6 also provides room for the expected critical

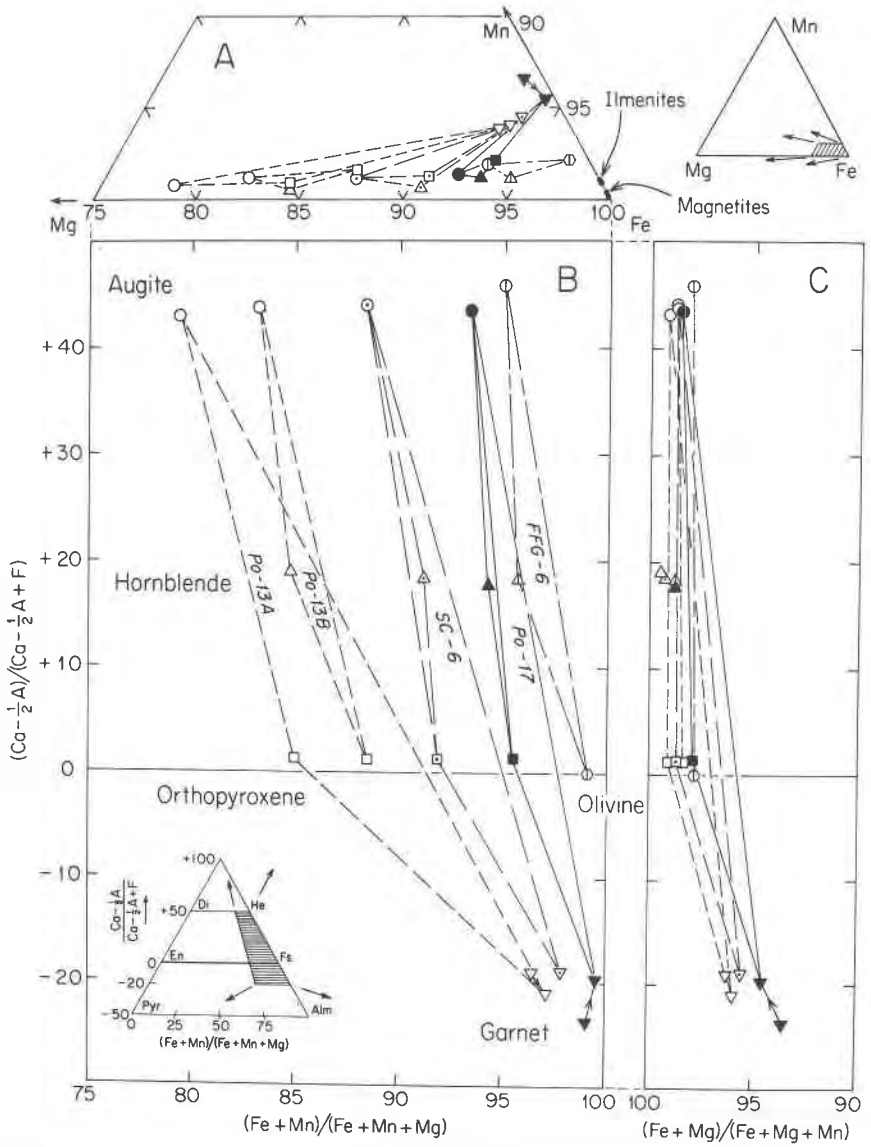

Fig. 5. Evaluation of ferromagnesian silicate assemblages in projection. In two garnet analyses from the same rock, arrow points from euhedral toward symplectic garnet. Specimen Po-13 contains two different coexisting pyroxene pairs. The more magnesian pyroxenes coexist with garnet, the more ferroan with hornblende. (A) Iron-rich corner of the triangle Fe–Mg–Mn showing distribution of these elements in coexisting silicates and oxides. (B) Rectangular plagioclase projection of composition of coexisting ferromagnesian silicates in terms of the ratios (Ca − 1/2A)/(Ca − 1/2A + F) and (Fe + Mn)/(Fe + Mn + Mg) where A = Al + Fe^{3+} + 2Ti + Cr − Na − K and F = Fe + Mn + Mg −Ti. Should Fe and Mn truly behave as isomorphous components, then under one set of conditions and in equilibrium with one plagioclase composition, there should be only a single orthopyroxene–augite–garnet three-phase field, not three as shown. Hornblende occurs as a fourth phase in two out of the three. (C) Rectangular plagioclase projection similar to (B) but in which the F component is displayed in terms of the ratio (Fe + Mg)/(Fe + Mg + Mn). Tie lines to hornblende compositions omitted for simplicity. This illustrates the determining role of Mn in the occurrence of garnet in these rocks, and shows that the overlapping positions of the three orthopyroxene–augite–garnet assemblages with respect to Mn are a function of Fe/Mg ratio.

but very narrow four-phase volume orthopyroxene–augite–garnet–olivine, a maximum phase assemblage for this system. Figures 5c and 6 provide scope for consideration of reactions by which the field of augite + garnet expands at the expense of orthopyroxene (+plagioclase) for rocks of a wide variety of Fe/Mg ratios. An essential feature of such reactions is the extension of garnet compositions in this assemblage toward the Fe + Mg face of the system.

The problem resolution provided above does not

assist with hornblende, which appears as a *fourth* ferromagnesian silicate in each orthopyroxene–augite–garnet assemblage, in each case positioned close to the orthopyroxene–augite tie line, but consistently on the Mn-poor side. Hornblende, of course, contains major amounts of additional components Fe^{3+}, Ti^{4+}, and K, but it is essentially saturated with these due to the presence of magnetite, ilmenite, and K-feldspar, hence these components cannot explain the presence of hornblende. It seems, on balance, to be due to the behavior of H_2O or perhaps F and Cl as determining inert components rather than perfectly mobile components in this seemingly very dry environment. The location of the hornblende analytical points, even with maximum Fe^{3+} correction, almost directly on pyroxene tie lines is another problem, because hornblende compositions usually project on the magnesian sides of pyroxene tie lines (see for example Ashwal, 1974). However, this problem may be more apparent than real, because slight Fe/Mg fractionation between pyroxenes and hornblende might be obscured in these extremely Fe-rich compositions.

Hornblende and its dehydration products

The Fe-rich pyroxene rocks provide a valuable opportunity to study the relations between hornblende and its anhydrous breakdown products, both ferromagnesian minerals and feldspars. This is done conveniently by expansion of the ACF triangle into an NaACF tetrahedron, in effect putting back the Na + K originally subtracted from A, and permitting direct portrayal of compositions of plagioclase and orthoclase. This may be converted to a more useful two-dimensional view by projection using orthopyroxene at the F apex as an excess phase, as shown in Figure 7. Such a projection from orthopyroxene, in effect from Fe + Mn + Mg, is easy to justify for orthopyroxene–augite–garnet assemblages representing bulk compositions within the triangular prismatic volume of Figure 6. Thus, in Figure 7 augite is represented as a calcic phase, garnet as aluminous. If Na and K are now imagined as being separate apices of a tetrahedron, then the assemblage plagioclase–orthoclase–augite–garnet (+ quartz + orthopyroxene) can be thought of as forming a four-phase volume of anhydrous breakdown products within which the compositions of hornblendes will plot. The topologic relations in Figure 7 show that the main breakdown products of these hornblendes would be plagioclase, orthoclase, and augite (+ orthopyroxene, − quartz + ilmenite, + magnetite), but that a small amount of

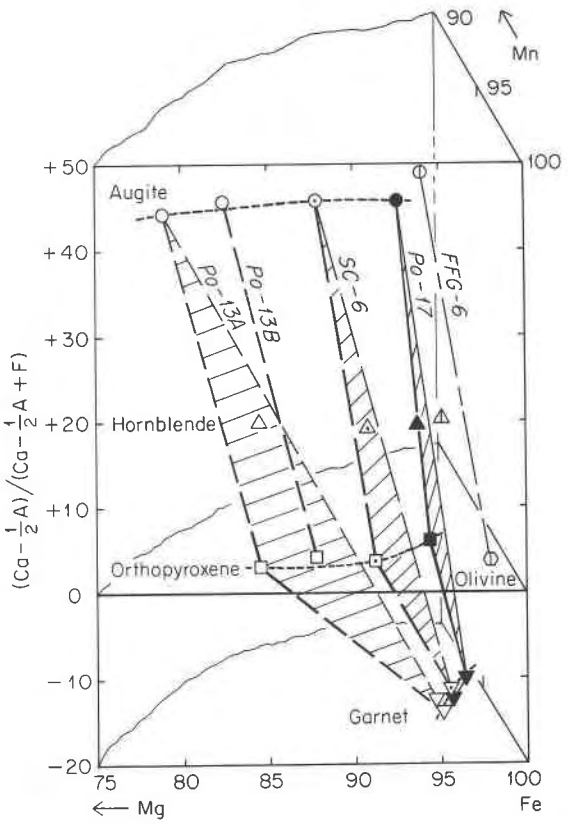

Fig. 6. The three parts of Fig. 5 combined in a three-dimensional plagioclase projection in which the components Mg, Fe, and Mn are all treated separately. Tie lines to hornblende are omitted for simplicity. Three orthopyroxene–augite–garnet tie planes define a triangular prismatic volume of bulk compositions that could contain this assemblage under identical conditions. The augite–olivine tie line lies outside this volume but helps to visualize the hypothetical position of a critical orthopyroxene–augite–garnet–olivine four phase volume. The two-phase tie line orthopyroxene–augite in assemblage Po-13B without garnet appears to violate the three-phase prismatic volume slightly, which could be due to late equilibration with Mn-poor hornblende.

garnet should also be produced. A view downward from the A apex of this imagined tetrahedron onto the Ca,Na,K base would look as in Figure 8. Figure 8 demonstrates in dramatic fashion that breakdown of these hornblendes would produce, in addition to orthopyroxene and minor garnet, sodium-bearing augite and feldspar which is *nearly equal* in amounts of oligoclase and orthoclase.

Conditions of formation

Figure 9 is a *P–T* diagram on which are plotted results of experiments bearing on the stability of iron-rich pyroxenes. The reaction $FeSiO_3$ (Fs_{100}) = Fe_2SiO_4 + SiO_2 from 750° to 1100°C is from Lindsley (1965)

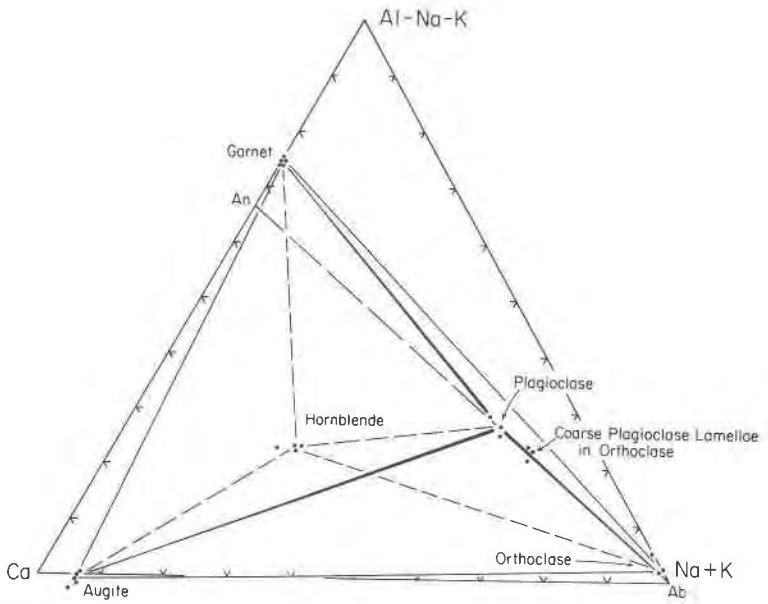

Fig. 7. Orthopyroxene projection in the tetrahedron Ca, Al–Na–K, Na+K, Mg+Fe+Mn onto the plane Ca, Al–Na+K, Na+K showing distribution of Ca, Al and alkalies in coexisting augite, hornblende, garnet, and feldspars from the three specimens from the Mt. Marcy quadrangle. All minerals show great regularity. Feldspar compositions shown include host plagioclase, coarse lamellae in orthoclase, and orthoclase. Hornblende lies within a triangle bounded by augite, garnet, and feldspars, and, if Na and K are treated separately, within a tetrahedron augite–garnet–plagioclase–orthoclase. This shows that the terminal reaction for hornblende is of the form: hornblende + quartz → orthopyroxene + augite + plagioclase + orthoclase + garnet(minor) (+ ilmenite + magnetite).

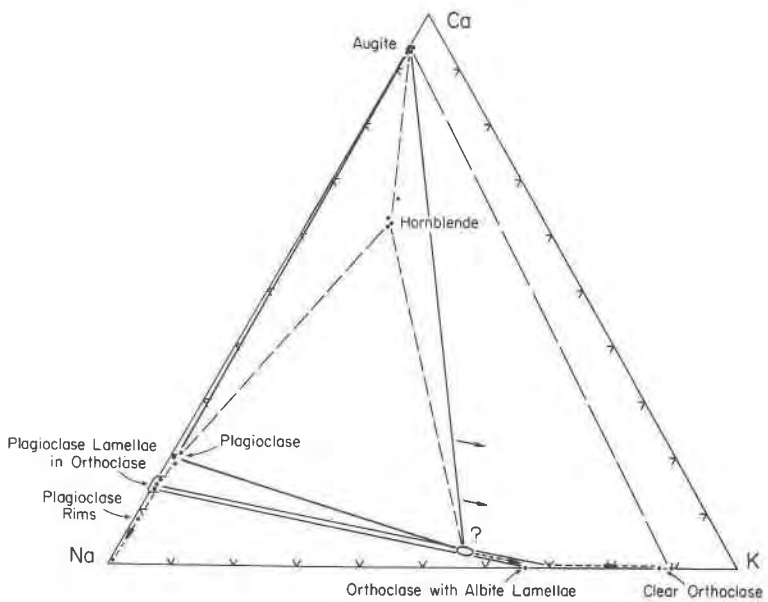

Fig. 8. Distribution of Ca,Na,K in coexisting augite, hornblende, and feldspars. A view from the Al–Na–K apex onto the base of an expanded tetrahedron as described under Fig. 7 Complex evolution of feldspar is illustrated. At earliest high temperature stage plagioclase An_{18-20} coexisted with sodic-calcic orthoclase (indicated "?"). This orthoclase exsolved coarse lamellae of composition An_{14-15}, thus depleting the host in nearly all Ca. Remaining orthoclase, Or_{65-70}, then exsolved nearly pure albite, driving host composition to Or_{88-90}. Much exsolved albite moved out of orthoclase hosts and formed thin albite rims on plagioclase host grains. Figure also demonstrates graphically that orthoclase is as important as plagioclase in the dehydration products of these Fe-rich hornblendes.

and Smith (1971b). Also shown are the experimental determinations of this reaction by Bohlen *et al.* (1978) and a calculated slope suggested by Wood and Strens (1971). A series of isopleths at 900°C indicate the compositions of orthopyroxenes in equilibrium with olivine and quartz in the system $MgSiO_3$–$FeSiO_3$ extrapolated directly from Smith (1971b), as well as Smith's data for Fs_{75} at 625°C. The figure also shows the lower temperature stability of pigeonite on the join hedenbergite$_{85}$–ferrosilite$_{85}$ as determined by Smith (1972) at 15–16 kbar and extrapolated to lower pressure[8]. Insets near this equilibrium show interpreted isothermal sections of the Fe-rich side of the pyroxene quadrilateral above and below this pigeonite equilibrium. Insets on the 650° isotherm illustrate *in exaggerated form* the *possible* effects of Ca-saturation due to the presence of augite in expanding the stability of orthopyroxene toward more Fe-rich compositions. Near 6 kbar, Ca-free orthopyroxene Fs_{85} is shown coexisting with olivine, but more Fe-rich Ca-bearing orthopyroxene occurs with augite and olivine. Near 8 kbar, Ca-free orthopyroxene Fs_{91} is shown coexisting with olivine, but the pure Fe–Ca endmember orthopyroxene coexists with augite.

Interpreting the Adirondack specimens in terms of the experimental data requires estimates of temperature of formation and estimates of the effects of minor-element substitutions on the natural material as compared to the simpler experimental systems. As far as is known, none of the iron-rich felsic rocks considered here contains evidence of ever having had primary pigeonite, although some metamorphosed anorthosites and gabbroic rocks of the anorthositic series from the same area do contain relics of inverted pigeonite. Thus, the upper temperature limit is the pigeonite reaction given in Figure 9. Because the compositions of the coexisting pyroxenes lie close to the hedenbergite–ferrosilite join, the Wo content of the augites can be projected into that join, and the experimental work of Lindsley and Munoz (1969) on the hedenbergite–ferrosilite join at 20 kbar can be used to estimate temperature. If X-ray data are used to reconstruct original high-temperature metamorphic augite compositions, then according to two different chemical criteria, the values of Wo 37 and Wo 39 are obtained. These Wo values yield temperature estimates of 790°C and 760°C respectively. The present augite host compositions, expressed alternatively as Wo 43.7 or Wo 45.7 (ignoring the fact that part of the exsolution was of pigeonite, not orthopyroxene), yield temperature estimates of 660°C and 600°C respectively for the episode of exsolution. Moreover, in an 810°C isotherm for coexisting augite and orthopyroxene in the quadrilateral, Lindsley *et al.* (1974) determined, with a large degree of uncertainty, a generalized $K_{D\ Fe-Mg}^{Opx-Cpx}$ of 0.690. This compares to values of 0.642 to 0.681 for host pyroxene pairs in this study (Table 4), suggesting a temperature lower than 810° for exsolution of the Adirondack rocks. The *pattern* of fine exsolution lamellae suggests exsolution may have taken place near 600°C (Robinson *et al.*, 1977). On these bases, the temperature of metamorphism of the Mount Marcy rocks is believed to have been no higher than 800°C nor lower than 600°C near the peak of metamorphism.

It is very difficult to make quantitative estimates of the effect of minor elements such as Ca, Mn, Zn, Na, Al, *etc.*, on the stability of orthopyroxene. The stability of orthopyroxene will be enhanced relative to that of olivine plus quartz by the presence of any of the above listed elements, because they are all partitioned preferentially into orthopyroxene. Of all the minor elements, the two most important are Ca and Mn. The presence of Ca should have an effect in stabilizing orthopyroxene to lower pressure, but only until the system reaches saturation with augite, as shown in insets in Figure 9. Mn has a pressure-lowering effect similar to that of Mg but of much smaller magnitude, as indicated by the fractionation of Fe, Mg, and Mn between olivine and orthopyroxene. Analyses of Huntington (1975) and Berg (1977) as well as preliminary data on a fayalite–ferrosilite–augite syenite (quartz-free) collected by Lewis Ashwal from the Paradox Lake quadrangle (number in parentheses) indicate that while $K_{D\ Fe-Mg}^{Opx-Oliv}$ is in the range 0.2–0.35 (0.323), the fractionation of Mn is much less: $K_{D\ Fe-Mn}^{Opx-Oliv}$ = 0.63–0.95 (0.823). Since it is not possible to assess quantitatively the effects of these minor components, it seemed best in this case to calculate the orthopyroxene ferrosilite content in two extreme ways. The first was to assume that the effect of minor elements is nil, and therefore to use the ratio Fe/(Fe + Mg) in applying the experimental calibration. The second was to assume that the effect of all minor components is the same as Mg and therefore to apply the ratio $Fe^{2+}/2.00$ (equivalent to the absolute molecular proportion of $Fe_2Si_2O_6$) to the experimental data. It must be remembered that these approximations are *extreme*, since it is almost certain that the effect of minor elements is neither nil nor the same as Mg. These extreme approximations, however, should serve to bracket the best value.

[8] D. H. Lindsley (personal communication, 1977) favors a temperature some 50–75° lower for this equilibrium at 15–16 kbar.

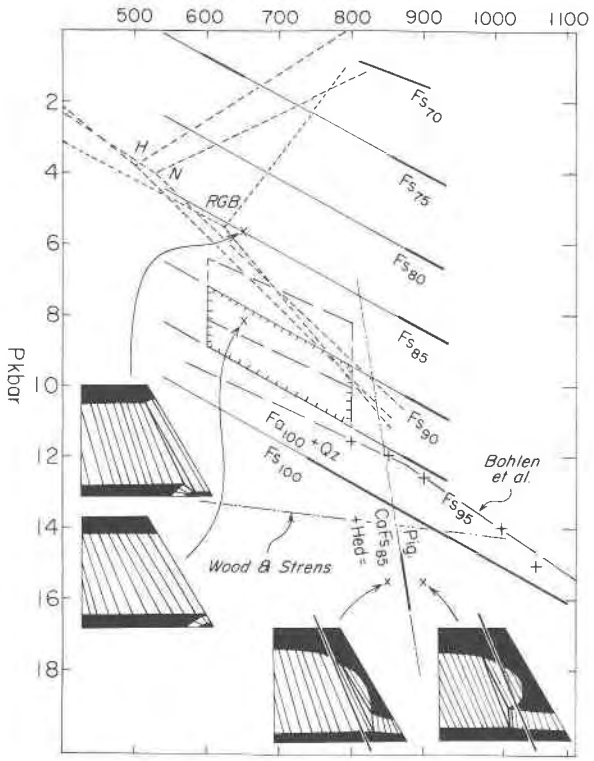

Fig. 9. *P–T* diagram with isopleths showing the compositions of orthopyroxene in equilibrium with olivine and quartz, based on experimental work of Lindsley (1965) and Smith (1971b) in the system $MgSiO_3$–$FeSiO_3$. Determination of Fs_{100} isopleth by Bohlen *et al.* (1978) and a calculation of its position by Wood and Strens (1971) are also shown, the former with an inflection consistent with the high–low quartz inversion. Also shown are the low temperature stability of pigeonite on the join hedenbergite$_{85}$–ferrosilite$_{85}$ as determined by Smith (1972) and the stabilities of the Al_2SiO_5 polymorphs based on Richardson *et al.* (1969), Newton (1966), and Holdaway (1971). Outlined areas indicate brackets for minimum pressure estimates for metamorphism of Mt. Marcy orthoferrosilite according to data of Smith (hachures) or of Bohlen *et al.* (long dashed). See text for detailed interpretation.

In order to estimate pressures for the Adirondacks, the calculated ferrosilite contents of orthopyroxenes have been applied to the isopleths of Smith (1971b) on Figure 9. The Smith calibration was used rather than the Wood and Strens calibration because the Fs_{100} curve of Smith is in reasonable agreement with the Fs_{100} curve of Bohlen *et al.* (1978), especially considering Smith's suggestion that his pressures are probably slightly high due to the mechanical behavior of the solid-media apparatus.

The ferrosilite content of the most iron-rich orthopyroxene of this study, Po-17, is calculated to be Fs 95 and Fs 90 respectively, using the two extreme calculation methods. If equilibration occurred at 800°C, then *minimum* pressure was 9 kbar and could have been as high as 11 kbar. Equilibration at 600°C implies *minimum* pressure of 7 kbar to 9 kbar (Table 9). These limiting minimum pressure values based on experimental data of Smith (1971b) are outlined on Figure 9, together with adjusted values estimated from the Fs_{100} experiments of Bohlen *et al.* (1978). Similar reasoning based on optical data for the eulite-bearing (Fs 88) specimen FFG-2 from near Wanakena, Cranberry Lake quadrangle, yields the minimum pressure estimates given in Table 9.

On the other hand, composition of olivine in the

Table 9. Estimates of pressure of metamorphism of selected Adirondack rocks*

	"Fs"	600°C	800°C
Estimates of minimum pressure (kbar) based on orthopyroxene composition in olivine-free assemblage.			
Po-17, Mt. Marcy quad., probe analyses			
Fe/(Fe + Mg)	.95	9	11
$Fe^{2+}/2.00$	.90	7	9
FFG-2, Cranberry Lake quad., optical estimates			
Fe/(Fe + Mg)	.88	6.5	9
$Fe^{2+}/2.00$	.84	4.5	7
Estimates of maximum pressure (kbar) based on olivine-augite assemblage where "hypothetical orthopyroxene" composition has been estimated.			
	"Fs"	600°C	800°C
FFG-6, Cranberry Lake quad., probe analyses			
Fe/(Fe + Mg)	.97	9.5	12
$Fe^{2+}/2.00$	.91	7.5	10
AF-1A, Ausable Forks quad., optical estimates			
Fe/(Fe + Mg)	.97	9.5	12
$Fe^{2+}/2.00$	.91	7.5	10

**To accord with the experiments of Bohlen et al. (1978) these values should be adjusted approximately -0.8 kbar at 600°C and -1.2 kbar at 800°C.*

orthopyroxene-free rock FFG-6 can be used to estimate *maximum* pressure of metamorphism at Wanakena. Based upon estimates of olivine–orthopyroxene fractionation, we estimate that olivine Fa 99 could coexist at higher pressures with orthopyroxene having $Fe/(Fe + Mg) = 0.97$ and $Fe^{2+}/2.00 = 0.91$. This hypothetical orthopyroxene composition, applied to the isopleths of Figure 9, yields *maximum* pressures as indicated in Table 9. Similar reasoning based on optical data for the olivine–augite–microperthite gneiss AF-1A from the Ausable Forks quadrangle, 30 km northeast of Pitchoff Mountain, gives identical maximum pressures (Table 9). Had either of these olivine-bearing specimens been obtained from the same locality as Po-17, then metamorphic conditions for the Mt. Marcy quadrangle would have been completely bracketed by four *P–T* points (Fig. 9): 7 and 9.5 kbar at 600°C, and 9 and 12 kbar at 800°C. Any revision in the pressures of Smith's (1971b) experimental calibration (Bohlen *et al.*, 1978) would cause proportional change of these pressure estimates at 600° and 800°C (see Table 9). Comparison of these brackets with experimental data on the Al_2SiO_5 polymorphs (Fig. 9) suggests metamorphism in the Mt. Marcy area took place near the high-pressure stability limit of sillimanite or in the kyanite zone.

Appendix—localities of analyzed specimens

Po-13 Near northeastern summit of Pitchoff Mountain, elevation 3471 feet, northern part of Mt. Marcy quadrangle.

SC-6 On east side of ski slope on Scott's Cobble, elevation 2300 feet, northernmost part of Mt. Marcy quadrangle.

PO-17 About 1 mile east of Highway 73, along a trail which is now a continuation of Old Military Road, elevation 2300 feet, Mt. Marcy quadrangle.

FFG-2 On the southwest side of road from Benson Mines to Inlet, near the road junction at 1695 feet, west-central Cranberry Lake quadrangle.

FFG-6 Road cuts on Route 3, about 4 miles east of Benson Mines near the junction of road to Wanakena, Cranberry Lake quadrangle.

AF-1A From a small abandoned quarry about 7/8 mile east-northeast of Ausable Forks, Ausable Forks quadrangle.

Acknowledgements

Field work, optical work, electron probe analyses, computation, and manuscript preparation were supported by NSF grant GA-31989 (to Jaffe and Robinson). Lattice parameters for orthoferrosilite sample Po-17 were determined by Malcolm Ross at the U.S. Geological Survey. Leo M. Hall collected samples FFG-2 and FFG-6 from the Cranberry Lake quadrangle, and Lewis D. Ashwal collected sample AF-1A from the Ausable Forks quadrangle. Elizabeth B. Jaffe participated in the mapping of the Mt. Marcy quadrangle. Mrs. Marie Litterer drafted Figure 1 and lettered Figures 2–9. The manuscript was typed by Maureen Burns. Constructive reviews of the manuscript were provided by C. V. Guidotti, Cornelis Klein, Jr., D. H. Lindsley, and Douglas Smith. To each of these persons and institutions we express our grateful acknowledgment.

References

Albee, A. L. and L. Ray (1970) Correction factors for electron probe microanalysis of silicates, oxides, carbonates, phosphates, and sulfates. *Anal. Chem., 42,* 1408–1914.

Ashwal, L. D. (1974) Metamorphic hydration of augite–orthopyroxene monzodiorite to hornblende granodiorite gneiss, Belchertown batholith, west-central Massachusetts. *Contrib. No. 18, Geology Department, University of Massachusetts, Amherst.*

Bence, A. E. and A. L. Albee (1968) Empirical correction factors for the electron microanalysis of silicates and oxides. *J. Geol., 76,* 382–403.

Berg, J. H. (1977) Regional geobarometry in the contact aureoles of the anorthositic Nain Complex, Labrador. *J. Petrol., 18,* 399–430.

Bohlen, S. R., A. L. Boettcher and E. J. Essene (1978) Experimental reinvestigation of ferrosilite–fayalite–quartz stability (abstr.). *EOS, 59,* 402.

Bonnichsen, B. (1969) Metamorphic pyroxenes and amphiboles in the Biwabik Iron Formation, Dunka River area, Minnesota. *Mineral. Soc. Am. Spec. Pap., 2,* 217–239.

Bowen, N. L. (1935) "Ferrosilite" as a natural mineral. *Am. J. Sci., 30,* 481–494.

——— and J. F. Schairer (1932) The system FeO–SiO_2. *Am. J. Sci., 24,* 177–213.

Bown, M. G. (1965) Reinvestigation of clinoferrosilite from Lake Naivasha, Kenya. *Mineral. Mag., 34,* 66–70.

Boyd, F. R. (1970) Garnet peridotites and the system $CaSiO_3$–$MgSiO_3$–Al_2O_3. *Mineral. Soc. Am. Spec. Pap., 3,* 63–75.

Buddington, A. F. (1969) Adirondack anorthositic series. In Y. W. Isachsen, Ed., *Origin of Anorthosites and Related Rocks,* p. 215–231. *N. Y. State Mus. Sci. Service Mem. 18.*

——— (1972) Differentiation trends and parental magmas for anorthosite and quartz mangerite series, Adirondacks, New York. *Geol. Soc. Am. Mem., 132,* 477–488.

——— and B. F. Leonard (1953) Chemical petrology and mineralogy of hornblendes in northwest Adirondack granitic rocks. *Am. Mineral., 38,* 891–902.

——— and ——— (1962) Regional geology of the St. Lawrence County magnetite district, northwest Adirondacks, New York. *U.S. Geol. Surv. Prof. Pap. 376.*

——— and D. H. Lindsley (1964) Iron-titanium oxide minerals and synthetic equivalents. *J. Petrol., 5,* 310–357.

Burnham, C. W. (1965) Ferrosilite. *Carnegie Inst. Wash. Year Book, 64,* 202–204.

Crosby, P. (1966) Meta-anorthosite of the Jay-Whiteface sheet, Ausable Forks–Lake Placid Quadrangles, northeastern Adirondacks, New York. *Field Trip Guidebook, George H. Hudson Symposium: Origin of Anorthosite, SUNY College, Plattsburgh, New York.*

Davis, B. T. C. (1969) Anorthositic and quartz syenitic series of the St. Regis quadrangle, New York. In Y. W. Isachsen, Ed., *Origin*

of Anorthosites and Related Rocks, p. 281–288. *N. Y. State Mus. Sci. Service Mem. 18.*

——— (1971) Bedrock geology of the St. Regis quadrangle, New York. *Map and Chart Ser. No. 16, N. Y. State Mus. Sci. Service, Albany.*

de Waard, D. (1970) The anorthosite–charnockite suite of rocks of Roaring Brook valley in the eastern Adirondacks (Marcy Massif). *Am. Mineral., 55,* 2063–2075.

Griffin, W. L. and K. S. Heier (1969) Paragenesis of garnet in granulite facies rocks, Lofoten-Vesteraalen, Norway. *Contrib. Mineral. Petrol. 23,* 89–116.

Henderson, C. M. B. (1968) Chemistry of hastingsitic amphiboles from the Marangudzi igneous complex, Southern Rhodesia. *Int. Mineral. Assn. Pap. Proc. 5th Gen. Mtg., Cambridge, 1966,* 291–304.

Holdaway, M. J. (1971) Stability of andalusite and the aluminum–silicate phase diagram. *Am. J. Sci., 271,* 97–131.

Huntington, J. C. (1975) Mineralogy and petrology of metamorphosed iron-rich beds in the Lower Devonian Littleton Formation, Orange Area, Massachusetts. *Contrib. No. 19, Geology Department, University of Massachusetts, Amherst.*

Jaffe, H. W., P. Robinson and R. J. Tracy (1974) Orthoferrosilite in Adirondack Gneiss (abstr.). *EOS, 55,* 468–469.

———, ———, ——— and M. Ross (1975) Orientation of pigeonite exsolution lamellae in metamorphic augite: correlation with composition and calculated optimal phase boundaries. *Am. Mineral., 60,* 9–28.

Kemp, J. F. (1921) Geology of the Mount Marcy quadrangle, New York. *N. Y. State Mus. Bull. 229–230.*

——— and H. L. Alling (1925) Geology of the Ausable quadrangle, New York. *N. Y. State Mus. Bull. 261.*

Klein, C. (1978) Regional metamorphism of Proterozoic iron-formation, Labrador Trough, Canada. *Am. Mineral., 63,* 898–912.

Leelanandam, C. (1970) Chemical mineralogy of hornblendes and biotites from the charnockitic rocks of Kondapalli, India. *J. Petrol., 11,* 475–505.

Lindsley, D. H. (1965) Ferrosilite. *Carnegie Inst. Wash. Year Book, 64,* 148–150.

———, B. T. C. Davis and I. D. MacGregor (1964) Ferrosilite ($FeSiO_3$): synthesis at high pressures and temperatures. *Science, 144,* 73–74.

———, H. E. King, Jr. and A. C. Turnock (1974) Compositions of synthetic augite and hypersthene coexisting at 810°C: application to pyroxenes from lunar highlands rocks. *Geophys. Res. Lett., 1,* 134–136.

——— and J. L. Munoz (1969) Subsolidus relations along the join hedenbergite–ferrosilite. *Am. J. Sci., 267A,* 295–324.

——— and D. Rumble, III (1977) Magnetite–ilmenite geothermometer–oxybarometer: an evaluation of old and new data. *EOS, 58,* 519.

———, J. Tso and J. V. Heyse (1974) Effect of Mn on the stability of pigeonite (abstr.). *Geol. Soc. Am. Abstracts with Programs, 6,* 846–847.

Newton, R. C. (1966) Kyanite–andalusite equilibrium from 700° to 800°C. *Science, 153,* 170–172.

Ormaasen, D. E. (1977) Petrology of the Hopen mangerite–charnockite intrusion, Lofoten, north Norway. *Lithos, 10,* 291–310.

Richardson, S. W., M. C. Gilbert and P. M. Bell (1969) Experimental determination of kyanite–andalusite and andalusite–sillimanite equilibria; the aluminum silicate triple point. *Am. J. Sci., 267,* 259–272.

Robinson, P. and H. W. Jaffe (1969) Chemographic exploration of amphibole assemblages from central Massachusetts and southwestern New Hampshire. *Mineral. Soc. Am. Spec. Pap., 2,* 251–274.

———, ———, M. Ross and C. Klein, Jr. (1971a) Orientation of exsolution lamellae in clinopyroxenes and clinoamphiboles: consideration of optimal phase boundaries. *Am. Mineral., 56,* 909–939.

———, M. Ross and H. W. Jaffe (1971b) Composition of the anthophyllite–gedrite series, comparisons of gedrite and hornblende, and the anthophyllite–gedrite solvus. *Am. Mineral., 56,* 1005–1041.

———, ———, G. L. Nord, Jr., J. R. Smyth and H. W. Jaffe (1977) Exsolution lamellae in augite and pigeonite: fossil indicators of lattice parameters at high temperature and pressure. *Am. Mineral., 62,* 857–873.

Smith, D. (1971a) Iron-rich pyroxenes. *Carnegie Inst. Wash. Year Book 69,* 285–290.

——— (1971b) Stability of the assemblage iron-rich orthopyroxene–olivine–quartz. *Am. J. Sci., 271,* 370–382.

——— (1972) Stability of iron-rich pyroxene in the system $CaSiO_3$–$FeSiO_3$–$MgSiO_3$. *Am. Mineral., 57,* 1413–1428.

Stout, J. H. (1971) Four coexisting amphiboles from Telemark, Norway. *Am. Mineral., 56,* 212–224.

Sueno, S., M. Cameron and C. T. Prewitt (1973) High temperature crystal chemistry of pyroxenes: the orthoferrosilite structure (abstr.). *Geol. Soc. Am. Abstracts with Programs, 5,* 829–30.

Wood, B. J. and R. G. Strens (1971) The orthopyroxene geobarometer. *Earth Planet. Sci. Lett., 11,* 1–6.

Manuscript received, February 22, 1977; accepted for publication, June 7, 1978.